Search for excited electrons in $p\bar{p}$ collisions at $\sqrt{s} = 1.96$ TeV

V.M. Abazov[36], B. Abbott[76], M. Abolins[66], B.S. Acharya[29], M. Adams[52], T. Adams[50], E. Aguilo[6], S.H. Ahn[31], M. Ahsan[60], G.D. Alexeev[36], G. Alkhazov[40], A. Alton[65,a], G. Alverson[64], G.A. Alves[2], M. Anastasoaie[35], L.S. Ancu[35], T. Andeen[54], S. Anderson[46], B. Andrieu[17], M.S. Anzelc[54], Y. Arnoud[14], M. Arov[61], M. Arthaud[18], A. Askew[50], B. Åsman[41], A.C.S. Assis Jesus[3], O. Atramentov[50], C. Autermann[21], C. Avila[8], C. Ay[24], F. Badaud[13], A. Baden[62], L. Bagby[53], B. Baldin[51], D.V. Bandurin[60], S. Banerjee[29], P. Banerjee[29], E. Barberis[64], A.-F. Barfuss[15], P. Bargassa[81], P. Baringer[59], J. Barreto[2], J.F. Bartlett[51], U. Bassler[18], D. Bauer[44], S. Beale[6], A. Bean[59], M. Begalli[3], M. Begel[72], C. Belanger-Champagne[41], L. Bellantoni[51], A. Bellavance[51], J.A. Benitez[66], S.B. Beri[27], G. Bernardi[17], R. Bernhard[23], I. Bertram[43], M. Besançon[18], R. Beuselinck[44], V.A. Bezzubov[39], P.C. Bhat[51], V. Bhatnagar[27], C. Biscarat[20], G. Blazey[53], F. Blekman[44], S. Blessing[50], D. Bloch[19], K. Bloom[68], A. Boehnlein[51], D. Boline[63], T.A. Bolton[60], G. Borissov[43], T. Bose[78], A. Brandt[79], R. Brock[66], G. Brooijmans[71], A. Bross[51], D. Brown[82], N.J. Buchanan[50], D. Buchholz[54], M. Buehler[82], V. Buescher[22], V. Bunichev[38], S. Burdin[43,b], S. Burke[46], T.H. Burnett[83], C.P. Buszello[44], J.M. Butler[63], P. Calfayan[25], S. Calvet[16], J. Cammin[72], W. Carvalho[3], B.C.K. Casey[51], N.M. Cason[56], H. Castilla-Valdez[33], S. Chakrabarti[18], D. Chakraborty[53], K.M. Chan[56], K. Chan[6], A. Chandra[49], F. Charles[19,‡], E. Cheu[46], F. Chevallier[14], D.K. Cho[63], S. Choi[32], B. Choudhary[28], L. Christofek[78], T. Christoudias[44,†], S. Cihangir[51], D. Claes[68], Y. Coadou[6], M. Cooke[81], W.E. Cooper[51], M. Corcoran[81], F. Couderc[18], M.-C. Cousinou[15], S. Crépé-Renaudin[14], D. Cutts[78], M. Ćwiok[30], H. da Motta[2], A. Das[46], G. Davies[44], K. De[79], S.J. de Jong[35], E. De La Cruz-Burelo[65], C. De Oliveira Martins[3], J.D. Degenhardt[65], F. Déliot[18], M. Demarteau[51], R. Demina[72], D. Denisov[51], S.P. Denisov[39], S. Desai[51], H.T. Diehl[51], M. Diesburg[51], A. Dominguez[68], H. Dong[73], L.V. Dudko[38], L. Duflot[16], S.R. Dugad[29], D. Duggan[50], A. Duperrin[15], J. Dyer[66], A. Dyshkant[53], M. Eads[68], D. Edmunds[66], J. Ellison[49], V.D. Elvira[51], Y. Enari[78], S. Eno[62], P. Ermolov[38], H. Evans[55], A. Evdokimov[74], V.N. Evdokimov[39], A.V. Ferapontov[60], T. Ferbel[72], F. Fiedler[24], F. Filthaut[35], W. Fisher[51], H.E. Fisk[51], M. Ford[45], M. Fortner[53], H. Fox[23], S. Fu[51], S. Fuess[51], T. Gadfort[71], C.F. Galea[35], E. Gallas[51], E. Galyaev[56], C. Garcia[72], A. Garcia-Bellido[83], V. Gavrilov[37], P. Gay[13], W. Geist[19], D. Gelé[19], C.E. Gerber[52], Y. Gershtein[50], D. Gillberg[6], G. Ginther[72], N. Gollub[41], B. Gómez[8], A. Goussiou[56], P.D. Grannis[73], H. Greenlee[51], Z.D. Greenwood[61], E.M. Gregores[4], G. Grenier[20], Ph. Gris[13], J.-F. Grivaz[16], A. Grohsjean[25], S. Grünendahl[51], M.W. Grünewald[30], J. Guo[73], F. Guo[73], P. Gutierrez[76], G. Gutierrez[51], A. Haas[71], N.J. Hadley[62], P. Haefner[25], S. Hagopian[50], J. Haley[69], I. Hall[66], R.E. Hall[48], L. Han[7], P. Hansson[41], K. Harder[45], A. Harel[72], R. Harrington[64], J.M. Hauptman[58], R. Hauser[66], J. Hays[44], T. Hebbeker[21], D. Hedin[53], J.G. Hegeman[34], J.M. Heinmiller[52], A.P. Heinson[49], U. Heintz[63], C. Hensel[59], K. Herner[73], G. Hesketh[64], M.D. Hildreth[56], R. Hirosky[82], J.D. Hobbs[73], B. Hoeneisen[12], H. Hoeth[26], M. Hohlfeld[22], S.J. Hong[31], S. Hossain[76], P. Houben[34], Y. Hu[73], Z. Hubacek[10], V. Hynek[9], I. Iashvili[70], R. Illingworth[51], A.S. Ito[51], S. Jabeen[63], M. Jaffré[16], S. Jain[76], K. Jakobs[23], C. Jarvis[62], R. Jesik[44], K. Johns[46], C. Johnson[71], M. Johnson[51], A. Jonckheere[51], P. Jonsson[44], A. Juste[51], E. Kajfasz[15], A.M. Kalinin[36], J.R. Kalk[66], J.M. Kalk[61], S. Kappler[21], D. Karmanov[38], P.A. Kasper[51], I. Katsanos[71], D. Kau[50], R. Kaur[27], V. Kaushik[79], R. Kehoe[80], S. Kermiche[15], N. Khalatyan[51], A. Khanov[77], A. Kharchilava[70], Y.M. Kharzheev[36], D. Khatidze[71], T.J. Kim[31], M.H. Kirby[54], M. Kirsch[21], B. Klima[51], J.M. Kohli[27], J.-P. Konrath[23], V.M. Korablev[39], A.V. Kozelov[39], D. Krop[55], T. Kuhl[24], A. Kumar[70], S. Kunori[62], A. Kupco[11], T. Kurča[20], J. Kvita[9,†], F. Lacroix[13], D. Lam[56], S. Lammers[71], G. Landsberg[78], P. Lebrun[20], W.M. Lee[51], A. Leflat[38], F. Lehner[42], J. Lellouch[17], J. Leveque[46], J. Li[79], Q.Z. Li[51], L. Li[49], S.M. Lietti[5], J.G.R. Lima[53], D. Lincoln[51], J. Linnemann[66], V.V. Lipaev[39], R. Lipton[51], Y. Liu[7,†], Z. Liu[6], A. Lobodenko[40], M. Lokajicek[11], P. Love[43], H.J. Lubatti[83], R. Luna[3], A.L. Lyon[51], A.K.A. Maciel[2], D. Mackin[81], R.J. Madaras[47], P. Mättig[26], C. Magass[21], A. Magerkurth[65], P.K. Mal[56], H.B. Malbouisson[3], S. Malik[68], V.L. Malyshev[36], H.S. Mao[51], Y. Maravin[60], B. Martin[14], R. McCarthy[73], A. Melnitchouk[67], L. Mendoza[8], P.G. Mercadante[5], M. Merkin[38], K.W. Merritt[51], J. Meyer[22,d], A. Meyer[21], T. Millet[20], J. Mitrevski[71], J. Molina[3], R.K. Mommsen[45], N.K. Mondal[29], R.W. Moore[6], T. Moulik[59], G.S. Muanza[20], M. Mulders[51], M. Mulhearn[71], O. Mundal[22], L. Mundim[3], E. Nagy[15], M. Naimuddin[51], M. Narain[78], N.A. Naumann[35], H.A. Neal[65], J.P. Negret[8], P. Neustroev[40], H. Nilsen[23], H. Nogima[3], S.F. Novaes[5], T. Nunnemann[25], V. O'Dell[51], D.C. O'Neil[6], G. Obrant[40], C. Ochando[16], D. Onoprienko[60], N. Oshima[51], J. Osta[56], R. Otec[10], G.J. Otero y Garzón[51], M. Owen[45], P. Padley[81], M. Pangilinan[78], N. Parashar[57], S.-J. Park[72], S.K. Park[31], J. Parsons[71], R. Partridge[78], N. Parua[55], A. Patwa[74], G. Pawloski[81], B. Penning[23], M. Perfilov[38], K. Peters[45], Y. Peters[26], P. Pétroff[16], M. Petteni[44], R. Piegaia[1], J. Piper[66], M.-A. Pleier[22], P.L.M. Podesta-Lerma[33,c], V.M. Podstavkov[51], Y. Pogorelov[56], M.-E. Pol[2],

P. Polozov[37], B.G. Pope[66], A.V. Popov[39], C. Potter[6], W.L. Prado da Silva[3], H.B. Prosper[50], S. Protopopescu[74], J. Qian[65], A. Quadt[22,d], B. Quinn[67], A. Rakitine[43], M.S. Rangel[2], K. Ranjan[28], P.N. Ratoff[43], P. Renkel[80], S. Reucroft[64], P. Rich[45], J. Rieger[55], M. Rijssenbeek[73], I. Ripp-Baudot[19], F. Rizatdinova[77], S. Robinson[44], R.F. Rodrigues[3], M. Rominsky[76], C. Royon[18], P. Rubinov[51], R. Ruchti[56], G. Safronov[37], G. Sajot[14], A. Sánchez-Hernández[33], M.P. Sanders[17], A. Santoro[3], G. Savage[51], L. Sawyer[61], T. Scanlon[44], D. Schaile[25], R.D. Schamberger[73], Y. Scheglov[40], H. Schellman[54], T. Schliephake[26], C. Schwanenberger[45], A. Schwartzman[69], R. Schwienhorst[66], J. Sekaric[50], H. Severini[76], E. Shabalina[52], M. Shamim[60], V. Shary[18], A.A. Shchukin[39], R.K. Shivpuri[28], V. Siccardi[19], V. Simak[10], V. Sirotenko[51], P. Skubic[76], P. Slattery[72], D. Smirnov[56], J. Snow[75], G.R. Snow[68], S. Snyder[74], S. Söldner-Rembold[45], L. Sonnenschein[17], A. Sopczak[43], M. Sosebee[79], K. Soustruznik[9], B. Spurlock[79], J. Stark[14], J. Steele[61], V. Stolin[37], D.A. Stoyanova[39], J. Strandberg[65], S. Strandberg[41], M.A. Strang[70], M. Strauss[76], E. Strauss[73], R. Ströhmer[25], D. Strom[54], L. Stutte[51], S. Sumowidagdo[50], P. Svoisky[56], A. Sznajder[3], M. Talby[15], P. Tamburello[46], A. Tanasijczuk[1], W. Taylor[6], J. Temple[46], B. Tiller[25], F. Tissandier[13], M. Titov[18], V.V. Tokmenin[36], T. Toole[62], I. Torchiani[23], T. Trefzger[24], D. Tsybychev[73], B. Tuchming[18], C. Tully[69], P.M. Tuts[71], R. Unalan[66], S. Uvarov[40], L. Uvarov[40], S. Uzunyan[53], B. Vachon[6], P.J. van den Berg[34], R. Van Kooten[55], W.M. van Leeuwen[34], N. Varelas[52], E.W. Varnes[46], I.A. Vasilyev[39], M. Vaupel[26], P. Verdier[20], L.S. Vertogradov[36], M. Verzocchi[51], F. Villeneuve-Seguier[44], P. Vint[44], P. Vokac[10], E. Von Toerne[60], V. Vorwerk[21], M. Voutilainen[68,e], R. Wagner[69], H.D. Wahl[50], L. Wang[62], M.H.L.S Wang[51], J. Warchol[56], G. Watts[83], M. Wayne[56], M. Weber[51], G. Weber[24], L. Welty-Rieger[55], A. Wenger[42], N. Wermes[22], M. Wetstein[62], A. White[79], D. Wicke[26], G.W. Wilson[59], S.J. Wimpenny[49], M. Wobisch[61], D.R. Wood[64], T.R. Wyatt[45], Y. Xie[78], S. Yacoob[54], R. Yamada[51], M. Yan[62], T. Yasuda[51], Y.A. Yatsunenko[36], K. Yip[74], H.D. Yoo[78], S.W. Youn[54], J. Yu[79], A. Zatserklyaniy[53], C. Zeitnitz[26], T. Zhao[83], B. Zhou[65], J. Zhu[73], M. Zielinski[72], D. Zieminska[55], A. Zieminski[55,‡], L. Zivkovic[71], V. Zutshi[53], and E.G. Zverev[38]

(The DØ Collaboration)

[1]*Universidad de Buenos Aires, Buenos Aires, Argentina*
[2]*LAFEX, Centro Brasileiro de Pesquisas Físicas, Rio de Janeiro, Brazil*
[3]*Universidade do Estado do Rio de Janeiro, Rio de Janeiro, Brazil*
[4]*Universidade Federal do ABC, Santo André, Brazil*
[5]*Instituto de Física Teórica, Universidade Estadual Paulista, São Paulo, Brazil*
[6]*University of Alberta, Edmonton, Alberta, Canada,*
Simon Fraser University, Burnaby, British Columbia,
Canada, York University, Toronto, Ontario, Canada,
and McGill University, Montreal, Quebec, Canada
[7]*University of Science and Technology of China, Hefei, People's Republic of China*
[8]*Universidad de los Andes, Bogotá, Colombia*
[9]*Center for Particle Physics, Charles University, Prague, Czech Republic*
[10]*Czech Technical University, Prague, Czech Republic*
[11]*Center for Particle Physics, Institute of Physics,*
Academy of Sciences of the Czech Republic, Prague, Czech Republic
[12]*Universidad San Francisco de Quito, Quito, Ecuador*
[13]*LPC, Univ Blaise Pascal, CNRS/IN2P3, Clermont, France*
[14]*LPSC, Université Joseph Fourier Grenoble 1, CNRS/IN2P3,*
Institut National Polytechnique de Grenoble, France
[15]*CPPM, IN2P3/CNRS, Université de la Méditerranée, Marseille, France*
[16]*LAL, Univ Paris-Sud, IN2P3/CNRS, Orsay, France*
[17]*LPNHE, IN2P3/CNRS, Universités Paris VI and VII, Paris, France*
[18]*DAPNIA/Service de Physique des Particules, CEA, Saclay, France*
[19]*IPHC, Université Louis Pasteur et Université de Haute Alsace, CNRS/IN2P3, Strasbourg, France*
[20]*IPNL, Université Lyon 1, CNRS/IN2P3, Villeurbanne, France and Université de Lyon, Lyon, France*
[21]*III. Physikalisches Institut A, RWTH Aachen, Aachen, Germany*
[22]*Physikalisches Institut, Universität Bonn, Bonn, Germany*
[23]*Physikalisches Institut, Universität Freiburg, Freiburg, Germany*
[24]*Institut für Physik, Universität Mainz, Mainz, Germany*
[25]*Ludwig-Maximilians-Universität München, München, Germany*
[26]*Fachbereich Physik, University of Wuppertal, Wuppertal, Germany*
[27]*Panjab University, Chandigarh, India*
[28]*Delhi University, Delhi, India*
[29]*Tata Institute of Fundamental Research, Mumbai, India*
[30]*University College Dublin, Dublin, Ireland*

[31]Korea Detector Laboratory, Korea University, Seoul, Korea
[32]SungKyunKwan University, Suwon, Korea
[33]CINVESTAV, Mexico City, Mexico
[34]FOM-Institute NIKHEF and University of Amsterdam/NIKHEF, Amsterdam, The Netherlands
[35]Radboud University Nijmegen/NIKHEF, Nijmegen, The Netherlands
[36]Joint Institute for Nuclear Research, Dubna, Russia
[37]Institute for Theoretical and Experimental Physics, Moscow, Russia
[38]Moscow State University, Moscow, Russia
[39]Institute for High Energy Physics, Protvino, Russia
[40]Petersburg Nuclear Physics Institute, St. Petersburg, Russia
[41]Lund University, Lund, Sweden, Royal Institute of Technology and Stockholm University,
Stockholm, Sweden, and Uppsala University, Uppsala, Sweden
[42]Physik Institut der Universität Zürich, Zürich, Switzerland
[43]Lancaster University, Lancaster, United Kingdom
[44]Imperial College, London, United Kingdom
[45]University of Manchester, Manchester, United Kingdom
[46]University of Arizona, Tucson, Arizona 85721, USA
[47]Lawrence Berkeley National Laboratory and University of California, Berkeley, California 94720, USA
[48]California State University, Fresno, California 93740, USA
[49]University of California, Riverside, California 92521, USA
[50]Florida State University, Tallahassee, Florida 32306, USA
[51]Fermi National Accelerator Laboratory, Batavia, Illinois 60510, USA
[52]University of Illinois at Chicago, Chicago, Illinois 60607, USA
[53]Northern Illinois University, DeKalb, Illinois 60115, USA
[54]Northwestern University, Evanston, Illinois 60208, USA
[55]Indiana University, Bloomington, Indiana 47405, USA
[56]University of Notre Dame, Notre Dame, Indiana 46556, USA
[57]Purdue University Calumet, Hammond, Indiana 46323, USA
[58]Iowa State University, Ames, Iowa 50011, USA
[59]University of Kansas, Lawrence, Kansas 66045, USA
[60]Kansas State University, Manhattan, Kansas 66506, USA
[61]Louisiana Tech University, Ruston, Louisiana 71272, USA
[62]University of Maryland, College Park, Maryland 20742, USA
[63]Boston University, Boston, Massachusetts 02215, USA
[64]Northeastern University, Boston, Massachusetts 02115, USA
[65]University of Michigan, Ann Arbor, Michigan 48109, USA
[66]Michigan State University, East Lansing, Michigan 48824, USA
[67]University of Mississippi, University, Mississippi 38677, USA
[68]University of Nebraska, Lincoln, Nebraska 68588, USA
[69]Princeton University, Princeton, New Jersey 08544, USA
[70]State University of New York, Buffalo, New York 14260, USA
[71]Columbia University, New York, New York 10027, USA
[72]University of Rochester, Rochester, New York 14627, USA
[73]State University of New York, Stony Brook, New York 11794, USA
[74]Brookhaven National Laboratory, Upton, New York 11973, USA
[75]Langston University, Langston, Oklahoma 73050, USA
[76]University of Oklahoma, Norman, Oklahoma 73019, USA
[77]Oklahoma State University, Stillwater, Oklahoma 74078, USA
[78]Brown University, Providence, Rhode Island 02912, USA
[79]University of Texas, Arlington, Texas 76019, USA
[80]Southern Methodist University, Dallas, Texas 75275, USA
[81]Rice University, Houston, Texas 77005, USA
[82]University of Virginia, Charlottesville, Virginia 22901, USA and
[83]University of Washington, Seattle, Washington 98195, USA

(Dated: February 2, 2008)

We present the results of a search for the production of an excited state of the electron, e^*, in proton-antiproton collisions at $\sqrt{s} = 1.96$ TeV. The data were collected with the D0 experiment at the Fermilab Tevatron Collider and correspond to an integrated luminosity of approximately 1 fb^{-1}. We search for e^* in the process $p\bar{p} \to e^* e$, with the e^* subsequently decaying to an electron plus photon. No excess above the standard model background is observed. Interpreting our data in the context of a model that describes e^* production by four-fermion contact interactions and e^* decay via electroweak processes, we set 95% C.L. upper limits on the production cross section ranging from 8.9 fb to 27 fb, depending on the mass of the excited electron. Choosing the scale for contact

interactions to be $\Lambda = 1$ TeV, excited electron masses below 756 GeV are excluded at the 95% C.L.

PACS numbers: 12.60.Rc, 14.60.Hi, 12.60.-i, 13.85.Rm

An open question in particle physics is the cause of the observed mass hierarchy of the quark and lepton SU(2) doublets in the standard model (SM). One proposed explanation for the three generations is a compositeness model [1] of the known leptons and quarks. According to this approach, a quark or a lepton is a bound state of three fermions or of a fermion and a boson [2]. Due to the underlying substructure, compositeness models imply a large spectrum of excited states. The coupling of excited fermions to ordinary quarks and leptons, resulting from novel strong interactions, can be described by contact interactions (CI) with the effective four-fermion Lagrangian [3]

$$\mathcal{L}_{\rm CI} = \frac{g^2}{2\Lambda^2} j^\mu j_\mu,$$

where Λ is the compositeness scale and j_μ is the fermion current

$$j_\mu = \eta_L \, \bar{f}_L \gamma_\mu f_L + \eta'_L \, \bar{f}^*_L \gamma_\mu f^*_L + \eta''_L \, \bar{f}^*_L \gamma_\mu f_L$$
$$+ h.c. + (L \to R).$$

The SM and excited fermions are denoted by f and f^*, respectively; g^2 is chosen to be 4π, the η factors for the left-handed currents are conventionally set to one, and the right-handed currents are set to zero.

Gauge mediated transitions between ordinary and excited fermions can be described by the effective Lagrangian [3]

$$\mathcal{L}_{\rm EW} = \frac{1}{2\Lambda} \bar{f}^*_R \, \sigma^{\mu\nu}$$
$$\left[g_s f_s \frac{\lambda^a}{2} G^a_{\mu\nu} + g f \frac{\tau}{2} W_{\mu\nu} + g' f' \frac{Y}{2} B_{\mu\nu} \right] f_L + h.c.$$

where $G^a_{\mu\nu}$, $W_{\mu\nu}$, and $B_{\mu\nu}$ are the field strength tensors of the gluon, the SU(2) and U(1) gauge fields, respectively, and f_s, f and f' are parameters of order one.

For the present analysis, we consider single production of an excited electron e^* in association with an electron via four-fermion contact interactions, with the subsequent electroweak decay of the e^* into an electron and a photon (Fig. 1(a)). This decay mode leads to the fully reconstructable and almost background-free final state $ee\gamma$. With the data considered herein, collected with the D0 detector at the Fermilab Tevatron Collider in $p\bar{p}$ collisions at $\sqrt{s} = 1.96$ TeV, the largest expected SM background is from the Drell-Yan (DY) process $p\bar{p} \to Z/\gamma^* \to e^+e^-(\gamma)$, with the final state photon radiated by either a parton in the initial state or from one of the final state electrons. This background can be strongly suppressed by the application of suitable selection criteria. Other backgrounds are small.

Previous searches have found no evidence for the production of excited electrons, e.g. at the CERN LEP e^+e^-

[5] and the DESY HERA ep [4] colliders, in the context of models where the production of excited electrons proceeds via gauge interactions; however, the reach has been limited by the available center-of-mass energy to $m_{e^*} \lesssim 300$ GeV. Searches for quark-lepton compositeness via deviations from the Drell-Yan cross section at the Tevatron have excluded values of Λ of up to ≈ 6 TeV depending on the chirality [6]. The present analysis is complementary to those results in the sense that an exclusive channel and different couplings (η factors) are probed. The CDF collaboration has recently presented results [7] for the production of excited electrons which will be discussed later.
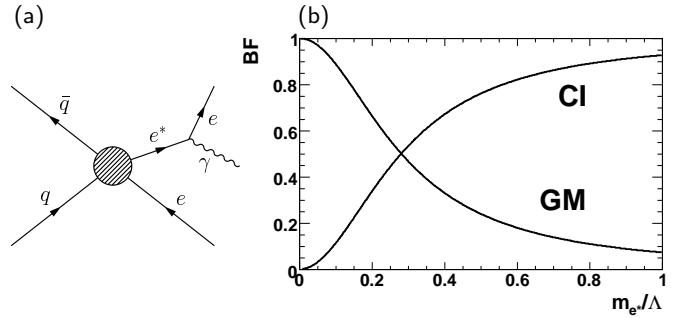

FIG. 1: (a) Four-fermion contact interaction $q\bar{q} \to e^*e$, and electroweak decay $e^* \to e\gamma$. (b) Relative contributions of decays via contact interactions and via electroweak interactions (GM) as a function of m_{e^*}/Λ.

For the simulation of the signal the PYTHIA event generator [8] is used, following the model of Ref. [3]. The branching fraction for the decay $e^* \to e\gamma$ normalized to all gauge particle decay modes is 30% for masses above 300 GeV; for smaller e^* masses it increases up to 73% at $m_{e^*} = 100$ GeV. Decays via contact interactions, not implemented in PYTHIA, contribute between a few percent of all decays for $\Lambda \gg m_{e^*}$ and 92% for $\Lambda = m_{e^*}$ [3] (see Fig. 1(b)). This is taken into account for the signal expectation. The leading order cross section calculated with PYTHIA is corrected to next-to-next-to-leading order (NNLO) using Ref. [9]; the corresponding correction factor varies between 1.37 and 1.42, depending on the invariant mass of the electron and the excited electron. The total width is greater than 1 GeV for 100 GeV $\leq m_{e^*} \leq 1000$ GeV, thus lifetime effects can be neglected. For the values of m_{e^*} and Λ studied here, the total width is always less than 10% of m_{e^*} [3].

The dominant SM background process at all stages of the selection is DY production of e^+e^- pairs. This background, as well as diboson (WW, WZ, ZZ) production, is simulated with the PYTHIA Monte Carlo (MC) program. The DY expectation (as well as $W \to e\nu$) is corrected using the NNLO calculation from Ref. [9]. For diboson production, the next-to-leading order cross

sections from Ref. [10] are used. Contributions from $t\bar{t}$ [11] and W boson production are found to be negligible. Monte Carlo events, both for SM and signal, are passed through a detector simulation based on the GEANT [12] package and reconstructed using the same reconstruction program as the data. The CTEQ6L1 parton distribution functions (PDFs) [13] are used for the generation of all MC samples.

The analysis is based on the data collected with the D0 detector [14] between August 2002 and February 2006, corresponding to an integrated luminosity of 1.01 ± 0.06 fb^{-1}. The D0 detector includes a central tracking system, which comprises a silicon microstrip tracker and a central fiber tracker, both located within a 2 T superconducting solenoidal magnet, and optimized for tracking and vertexing capability at pseudorapidities[1] $|\eta| < 2.5$. Three liquid argon and uranium calorimeters provide coverage out to $|\eta| \approx 4.2$: a central section (CC) covering $|\eta| \lesssim 1.1$, and two end calorimeters (EC). The electromagnetic section of the calorimeter has four longitudinal layers and transverse segmentation of 0.1×0.1 in $\eta - \phi$ space, except in the third layer, where it is 0.05×0.05. A muon system resides beyond the calorimetry, and consists of layers of tracking detectors and scintillation trigger counters before and after 1.8 T iron toroids. Luminosity is measured using scintillator arrays located in front of the EC cryostats, covering $2.7 < |\eta| < 4.4$. A three-level trigger system uses information from tracking, calorimetry, and muon systems to reduce the $p\bar{p}$ bunch crossing rate of 1.5 MHz to ≈ 100 Hz, which is written to tape.

Efficiencies for electron and photon identification and track reconstruction are determined from the simulation. To verify the simulation and to estimate systematic uncertainties, the efficiencies are also calculated from data samples, using $Z \rightarrow e^+e^-$ candidate events and other dilepton events for electrons and tracks. Small differences between the efficiency determinations from data and simulation are corrected in the simulation. We assume that the different response for electrons and photons in the calorimeter is properly modeled by the simulation. The transverse (with respect to the beam axis) momentum resolution of the central tracker and the energy resolution of the electromagnetic calorimeter are tuned in the simulation to reproduce the resolutions observed in the data using $Z \rightarrow \ell\ell$ ($\ell = e, \mu$) events.

The process $p\bar{p} \rightarrow e^*e$ with $e^* \rightarrow e\gamma$ leads to a final state with two highly energetic isolated electrons and a photon. First, the two electrons are identified as clusters of calorimeter energy with characteristic longitudinal and transverse shower shapes and at least 90% of the energy deposited in the electromagnetic section of
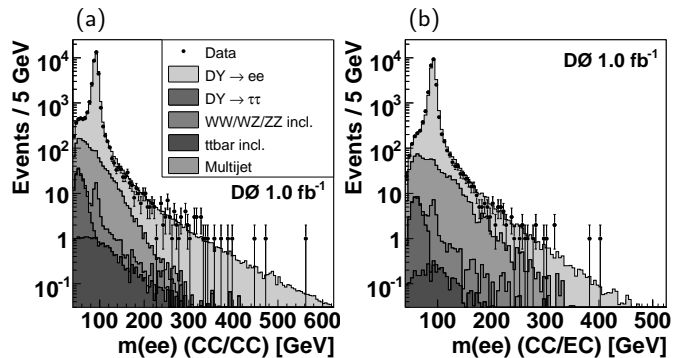

FIG. 2: Invariant dielectron mass distribution in the dielectron data sample compared to the SM expectation (a) for events with both electrons reconstructed in the CC and (b) for events in the CC/EC topology, for data (points with statistical uncertainties) and SM backgrounds (DY, diboson, $t\bar{t}$, and multijet production).

the calorimeter. Two electrons, with transverse energies $E_T > 25$ GeV and $E_T > 15$ GeV, are required. Both electrons are matched to tracks in the central tracking system, and we distinguish between CC ($|\eta| < 1.1$ with respect to the detector center) and EC ($1.5 < |\eta| < 2.5$) electrons. Events with the two electrons in opposite EC are rejected in order to suppress multijet background. The signal is expected to produce isolated electrons, therefore both electrons need to fulfill $\mathcal{I} \equiv (E_{\text{tot}}(0.4) - E_{\text{em}}(0.2))/E_{\text{em}}(0.2) < 0.2$, where $E_{\text{tot}}(0.4)$ and $E_{\text{em}}(0.2)$ denote the energies deposited in the calorimeter and deposited in only its electromagnetic section, respectively, in cones of size $\Delta\mathcal{R} = \sqrt{(\Delta\eta)^2 + (\Delta\phi)^2} = 0.4$ and 0.2. The electrons are required to be separated by $\Delta\mathcal{R} > 0.4$.

The events were collected with trigger conditions requiring one or two electrons detected in the calorimeters, with varying conditions depending on the E_T thresholds, the shower shape, tracks in the central tracking system, and number of electrons. The overall trigger efficiency is determined from independent data samples and is consistent with 100% for the signal after application of all selection criteria. The selected dielectron sample contains 62930 events, whereas 61900 ± 5700 events are expected from SM processes. The invariant dielectron mass distributions for CC/CC and CC/EC topologies are shown in Fig. 2. The largest SM contribution is DY production of e^+e^- pairs, followed by multijet production with misidentified electrons. The multijet background is estimated using a data sample where at least one of the electron candidates fails the shower shape requirements. This sample is then corrected as a function of E_T and η of the misidentified electrons in order to account for different misidentification rates in the CC and EC and the different trigger efficiency for misidentified electrons.

Next, a photon is identified in the event as an isolated cluster of calorimeter energy with at least 97% of its energy deposited in the electromagnetic section of the calorimeter (CC or EC). The isolation condition is $\mathcal{I} < 0.07$. The photon candidate E_T must be larger than

---

[1] The pseudorapidity η is defined as $\eta = -\ln\left[\tan(\theta/2)\right]$. We use the polar angle θ relative to the proton beam direction, and ϕ is the azimuthal angle, all measured with respect to the geometric center of the detector.
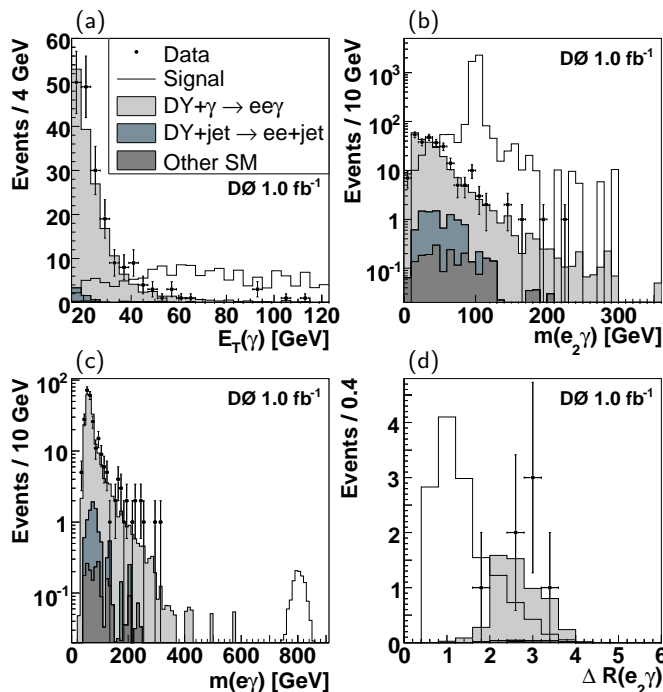
FIG. 3: For the $ee\gamma$ sample, (a) the photon E_T distribution, (b) the distribution of the $e_2\gamma$ invariant mass compared with the SM expectation and a possible e^* signal for $m_{e^*} = 100$ GeV; (c) the $e\gamma$ invariant mass for the $e\gamma$ combination closest to $m_{e^*} = 800$ GeV. In (d) the separation $\Delta R(e_2,\gamma)$ is shown after the cut on the invariant mass $m(e_2,\gamma) > 90$ GeV for $m_{e^*} = 100$ GeV. The signal corresponds to $\Lambda = 2$ TeV, 1 TeV, 1 TeV and 4 TeV in (a), (b), (c) and (d), respectively. All uncertainties are statistical only.

15 GeV, no track is allowed to be matched to the photon candidate in η and ϕ with a χ^2 probability of greater than 0.1%, and the sum of the transverse momenta of tracks within a hollow cone defined by $0.05 < \Delta R < 0.4$ around the photon direction has to be below 2 GeV to further ensure isolation. Additional shower shape criteria are imposed to increase the photon purity. The photon candidate is required to be separated from the electron candidates in the event by $\Delta R > 0.4$.

After this selection, 239 ± 36 events are expected from SM processes. Of these, 226 events are due to DY $\rightarrow e^+e^-$ with a genuine high E_T photon, followed by 7 events from DY $\rightarrow e^+e^- +$ jets, where a jet is misidentified as a photon. The absolute rate of the latter process has been determined from a data sample enriched in "fake" photons, applying the rate for such objects to be misidentified as photons as a function of E_T, and subtracting the true photon contribution [15]. Finally, about 4 and 2 events are expected from multijet and diboson production, respectively. In the data, 259 events are selected, compatible with the SM prediction. The photon E_T distributions for the data and SM background are shown in Fig. 3(a).

Additional selection criteria depending on the hypothetical e^* mass are applied to reduce the remaining SM

background. The following criteria have all been optimized to achieve the best expected upper limit on the production cross section. The e^* invariant mass can be reconstructed from one of the electrons and the photon. For $m_{e^*} < 300$ GeV, the lower E_T electron (e_2) is predominantly the decay electron. Alternatively, of the two possibilities to reconstruct the $e\gamma$ invariant mass, the value closest to the e^* candidate mass is chosen. The latter has been done for $m_{e^*} \geq 300$ GeV. Example mass distributions for the two chosen options to reconstruct the e^* candidate mass are shown in Figs. 3(b) and (c). The alternatives of single-sided mass cuts and a mass window are considered, leading to single-sided cuts for all values of m_{e^*}. Rejecting events with both electrons or the photon in the EC leads to a slightly better sensitivity; since for high values of m_{e^*} the SM backgrounds are extremely small, we have not applied these selection criteria for $m_{e^*} \geq 400$ GeV, in order to keep the search general beyond the specific model considered here. Finally, the separation $\Delta R(e_2,\gamma)$ between the lower E_T electron and the photon allows discrimination between signal and background for $m_{e^*} \leq 200$ GeV. This is illustrated in Fig. 3(d) for $m_{e^*} = 100$ GeV. All mass-dependent selection criteria are summarized in Table I.

TABLE I: Mass-dependent selection criteria. The second and the third columns show the lower mass cuts. The next two columns show if events with both electrons or the photon in the EC are kept, respectively, and in the last column the upper value for the separation between the second electron and the photon is given.

m_{e^*} [GeV]	$m(e_2,\gamma)$ [GeV]	$m(e\gamma)^{\text{closest}}$ [GeV]	EC/EC e	EC γ	$\Delta R(e_2,\gamma)$
100	> 90	–	no	no	< 1.8
200	> 165	–	no	no	< 3.3
300	–	> 285	no	no	any
400	–	> 370	yes	yes	any
500	–	> 445	yes	yes	any
600	–	> 515	yes	yes	any
700	–	> 600	yes	yes	any
800	–	> 705	yes	yes	any
900	–	> 800	yes	yes	any
1000	–	> 900	yes	yes	any

The final selection efficiency varies from 13% ($m_{e^*} = 100$ GeV) up to $\approx 33\%$ for higher values of m_{e^*}. In the data we find one event each for the $m_{e^*} = 200$ GeV mass hypothesis and for the $m_{e^*} = 300$ GeV mass hypothesis, respectively, and no events for other values of m_{e^*}, compatible with the SM expectation. This result is summarized in Table II.

The dominant systematic uncertainties are as follows. The uncertainty on the SM cross sections is dominated by the DY process and the uncertainty from the choice of PDF and renormalization and factorization scales [(3 $-$ 10)%]. Electron reconstruction and identification have an uncertainty of 2.5% per electron, and a $(1-4)\%$ uncertainty is assigned to the photon identification, depending

TABLE II: For different values of the e^* mass hypothesis, the
number of selected data events, the SM expectation including
statistical and systematic uncertainties, and the signal effi-
ciency.

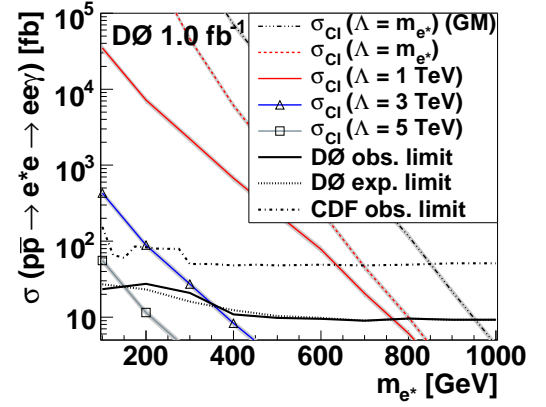| m_{e^*} [GeV]	Data	SM expectation	Signal eff. [%]
100	0	$0.33 \pm 0.09 \pm 0.03$	$13.2 \pm 0.6 \pm 1.3$
200	1	$0.52 \pm 0.16 \pm 0.05$	$16.5 \pm 0.6 \pm 1.6$
300	1	$0.32 \pm 0.12 \pm 0.03$	$22.2 \pm 0.7 \pm 2.2$
400	0	$0.26 \pm 0.11 \pm 0.03$	$28.3 \pm 0.8 \pm 2.8$
500	0	$0.12 \pm 0.08 \pm 0.01$	$31.5 \pm 1.0 \pm 3.1$
600	0	$(0.57 \pm 0.54 \pm 0.06) \times 10^{-1}$	$32.3 \pm 0.9 \pm 3.2$
700	0	$(0.82 \pm 0.37 \pm 0.09) \times 10^{-3}$	$34.3 \pm 1.1 \pm 3.4$
800	0	$(0.48 \pm 0.28 \pm 0.06) \times 10^{-3}$	$32.2 \pm 0.8 \pm 3.2$
900	0	$(0.17 \pm 0.17 \pm 0.02) \times 10^{-3}$	$33.2 \pm 0.8 \pm 3.3$
1000	0	$(0.17 \pm 0.17 \pm 0.03) \times 10^{-3}$	$33.3 \pm 0.9 \pm 3.3$

FIG. 4: The measured and expected limits on cross section
times branching fraction, compared to the contact interaction
model prediction for different choices of Λ. Also shown is the
prediction under the assumption that no decays via contact
interactions occur ("GM"), and the CDF result [7]. The the-
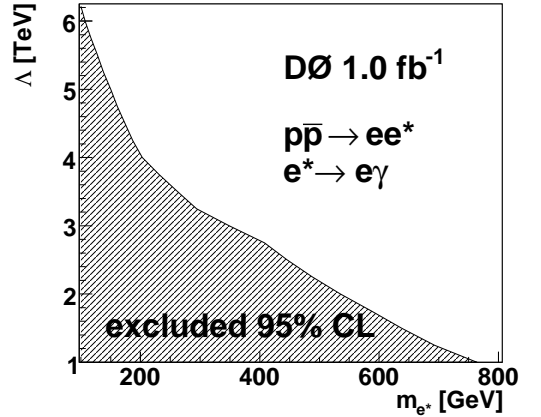oretical uncertainty of the model prediction is indicated by
shaded bands.

FIG. 5: The region in the $\Lambda - m_{e^*}$ plane excluded by the
present analysis.

on η and E_T. The trigger efficiency is $100^{+0}_{-3}\%$. The in-
tegrated luminosity is known to a precision of 6.1% [16].
The uncertainty on the number of background events due
to jets misidentified as photons is estimated to be 60%
of this particular background, from differences between
the expectation from the simulation and the independent
measurement from the data. A 25% uncertainty is de-
termined on the multijet background by comparing the
resulting multijet background estimate when using dif-
ferent criteria to select the multijet background sample;
after all selections, the multijet background is negligible.
The uncertainty on the signal cross section is estimated
to be 10%, consisting of PDF uncertainties and missing
higher order corrections.

Since the observed number of events is in agreement
with the SM expectation, we set 95% C.L. limits on the
e^* production cross section times the branching fraction
into $e\gamma$. A Bayesian technique [17] is used, taking into
account all uncertainties and treating them as symmetric
for simplicity. The resulting limit as a function of m_{e^*} is
shown in Fig. 4 together with predictions of the contact
interaction model for different choices of the scale Λ. For
$\Lambda = 1$ TeV ($\Lambda = m_{e^*}$), masses below 756 GeV (796 GeV)
are excluded. In Fig. 5, the excluded region in terms of
Λ and m_{e^*} is shown.

The CDF collaboration has recently searched [7] for
the production of excited electrons using a data sample
corresponding to an integrated luminosity of 202 pb^{-1},
but the CDF mass limit of $m_{e^*} > 879$ GeV at the 95%
C.L. for $\Lambda = m_{e^*}$ cannot be directly compared to ours for
two reasons. The e^* production cross section calculated
with the version of PYTHIA used in Ref. [7] is a factor of
two higher than in subsequent versions corrected by the
PYTHIA authors. Furthermore, in Ref. [7], it is assumed
that decays via contact interactions can be neglected,
while in our analysis such decays are taken into account
in the calculation of the branching fraction $e^* \rightarrow e\gamma$,
following Ref. [3]. Omitting contact interaction decays,
we would obtain a limit of $m_{e^*} > 946$ GeV for $\Lambda = m_{e^*}$

at the 95% C.L.[2]

In summary, we have searched for the production of
excited electrons in the process $p\bar{p} \rightarrow e^*e$ with $e^* \rightarrow e\gamma$, using about 1 fb^{-1} of data collected with the D0
detector. We find zero or one event in the data depending
on the mass of the hypothetical e^*, compatible with the
SM expectation. We set limits on the production cross
section times branching fraction as a function of m_{e^*}. For
a scale parameter $\Lambda = 1$ TeV, masses below 756 GeV are
excluded, representing the most stringent limit to date.

[2] Multiplying the theoretical prediction in addition by a factor of
two, the mass limit would increase to 989 GeV.

[a] Visitor from Augustana College, Sioux Falls, SD, USA.
[b] Visitor from The University of Liverpool, Liverpool, UK.
[c] Visitor from ICN-UNAM, Mexico City, Mexico.
[d] Visitor from II. Physikalisches Institut, Georg-August-University, Göttingen, Germany.
[e] Visitor from Helsinki Institute of Physics, Helsinki, Finland.
[†] Fermilab International Fellow.
[‡] Deceased.

[1] H. Terazawa, M. Yasue, K. Akama and M. Hayashi, Phys. Lett. B **112**, 387 (1982); F.M. Renard, Nuovo Cimento **A77**, 1 (1983); A. De Rujula, L. Maiani and R. Petronzio, Phys. Lett. B **140**, 253 (1984); E.J. Eichten, K.D. Lane and M.E. Peskin, Phys. Rev. Lett. **50**, 811 (1983).
[2] H. Terazawa, Y. Chikashige and K. Akama, Phys. Rev. D **15**, 480 (1977); Y. Ne'eman, Phys. Lett. B **82**, 69 (1979).
[3] U. Baur, M. Spira and P.M. Zerwas, Phys. Rev. D **42**, 815 (1990).
[4] C. Adloff *et al.* (H1 Collaboration), Phys. Lett. B **548**, 35 (2002); S. Chekanov *et al.* (ZEUS Collaboration), Phys. Lett. B **549**, 32 (2002).
[5] G. Abbiendi *et al.* (OPAL Collaboration), Phys. Lett. B **544**, 57 (2002); P. Achard *et al.* (L3 Collaboration), Phys. Lett. B **568**, 23 (2003); P. Abreu *et al.* (DELPHI Collaboration), Eur. Phys. J. C **8**, 41 (1999); R. Barate *et al.* (ALEPH Collaboration), Eur. Phys. J. C **4**, 571 (1998).
[6] B. Abbott *et al.* (D0 Collaboration), Phys. Rev. Lett. **82**, 4769 (1999).
[7] D. Acosta *et al.* (CDF Collaboration), Phys. Rev. Lett. **94**, 101802 (2005).
[8] T. Sjöstrand *et al.*, Comput. Phys. Commun. **135**, 238 (2001). PYTHIA version 6.3 is used throughout.
[9] R. Hamberg, W.L. van Neerven and T. Matsuura, Nucl. Phys. **B359**, 343 (1991); Erratum Nucl. Phys. **B644**, 403 (2002).
[10] J.M. Campbell and R.K. Ellis, Phys. Rev. D **60**, 113006 (1999); J.M. Campbell and R.K. Ellis, http://mcfm.fnal.gov/.
[11] N. Kidonakis and R. Vogt, Int. J. Mod. Phys. A **20**, 3171 (2005).
[12] R. Brun and F. Carminati, CERN Program Library Long Writeup W5013, 1994 (unpublished).
[13] J. Pumplin *et al.*, J. High Energy Phys. **0207**, 012 (2002); D. Stump *et al.*, J. High Energy Phys. **0310**, 046 (2003).
[14] V. Abazov *et al.* (D0 Collaboration), Nucl. Instrum. Methods Phys. Res., Sect. A **565**, 463 (2006).
[15] V. Abazov *et al.* (D0 Collaboration), Phys. Lett. B **653**, 378 (2007).
[16] T. Andeen *et al.*, Fermilab-TM-2365 (2007).
[17] I. Bertram *et al.* (D0 Collaboration), Fermilab-TM-2104 (2000).